



# Testing and analysis of the plastic scintillator units for LHAASO-ED

Ya-Ping Wang<sup>1,2,3</sup> · Chao Hou<sup>1,3</sup> · Xiang-Dong Sheng<sup>1,3</sup> · Shao-Hui Feng<sup>1,3</sup> · Hong-Kui Lv<sup>1,3</sup> · Jia Liu<sup>1,3</sup> · Jing Zhao<sup>1,3</sup> · Xiao-Peng Zhang<sup>1,3</sup> · Quan-Bu Gou<sup>1,3</sup>

Received: 16 March 2021 / Revised: 17 May 2021 / Accepted: 23 May 2021 / Published online: 24 August 2021  
© Institute of High Energy Physics, Chinese Academy of Sciences 2021

## Abstract

**Background** A total of 5195 electromagnetic particle detectors (EDs) are used in the 1-square-kilometer extensive air shower array (KM2A), which is a subarray of the Large High Altitude Air Shower Observatory (LHAASO).

**Purpose** As the detection sensitive medium of the EDs, more than 20,000 plastic scintillator units (BC-408), produced by Saint-Gobain, are used in LHAASO. It is important to monitor the light output of the scintillator units among the units.

**Method** To improve the efficiency, a sampling inspection scheme (misjudgment rate of less than 5%) was designed, and a batch test system was developed. Ten units of scintillator units can be measured at a time. The test system selects the single muon events of cosmic rays to measure the light output values of the plastic scintillator units.

**Results** The measurement has an uncertainty of less than 2%. By pretest calibration, the difference between different channels can be eliminated. The calibration was implemented approximately every 3 months, and the test system had been running stably for 28 months. By measuring the ratio of the signals of selected far and near probe events, the changes in the quality of different batches of plastic scintillator units can be demonstrated.

**Conclusions** The test system realized accurate measurement of the light output, and all batches satisfied the requirements of the experiment.

**Keywords** LHAASO · ED · Plastic scintillator unit · Light output

## Introduction

The Large High Altitude Air Shower Observatory (LHAASO) [1–3] is a hybrid extensive air shower array being built at 4410 meters at the Haizi Mountain, Daocheng site, Sichuan Province, China. As a subarray of LHAASO, KM2A consists of 5195 electromagnetic particle detectors (EDs) and 1188 muon detectors (MDs) [4]. The EDs are used for measuring the density and arrival time of secondary particles such as  $\gamma$ ,  $e^\pm$  and  $\mu^\pm$  in the extensive air shower (EAS) fronts that are initiated by primary cosmic rays (Fig. 1).

The inner view of an ED is shown in Fig. 2. There are 4 detection sensitive units, a photomultiplier tube (1.5-inch XP3960 PMT), electronics, a power system and a shell in each ED [5,6]. Each detection sensitive unit has one plastic scintillator unit (100 cm (length)  $\times$  25 cm (width)  $\times$  1 cm (thickness)) and twelve 2.7-m-long wavelength-shifting (WLS) fibers (BCF92SC,  $\Phi$  1.5 mm) [7]. Twelve WLS fibers are embedded in 24 grooves of the scintillator unit. All end faces of the 48 WLS fibers are bunched together and directly coupled to the photocathode of the PMT [8], which converts optical signals into electrical signals. The signals of the anode and dynode of the PMT are processed with electronics [9] to obtain ADC and TDC count values. The White Rabbit (WR) switch is used to obtain the time accuracy within 0.5 ns. The power system supplies low voltages to electronics and a high voltage to the PMT. Four 5-mm-thick lead plates that can convert  $\gamma$  into electron pairs are placed on top of the detection sensitive units. The performance of ED can be found elsewhere [10].

More than 20,000 plastic scintillator units will be used in the construction of EDs. Therefore, in this paper, a sampling

✉ Ya-Ping Wang  
wangyaping@ihep.ac.cn

<sup>1</sup> Key Laboratory of Particle Astrophysics & Experimental Physics Division & Computing Center, Institute of High Energy Physics, Chinese Academy of Sciences, Beijing 100049, China

<sup>2</sup> University of Chinese Academy of Sciences, Beijing 100049, China

<sup>3</sup> TIANFU Cosmic Ray Research Center, Chengdu, Sichuan, China

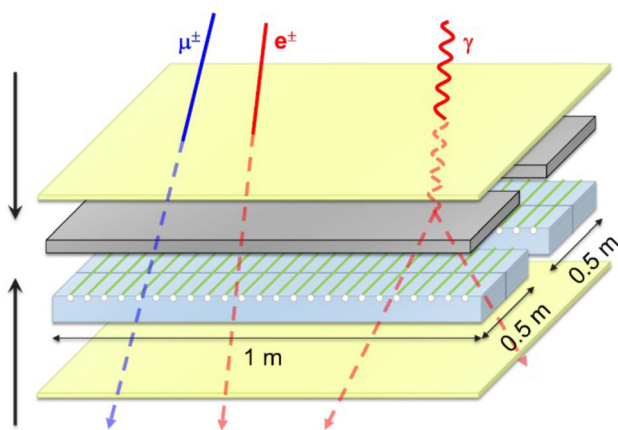


Fig. 1 Sketch picture of an ED

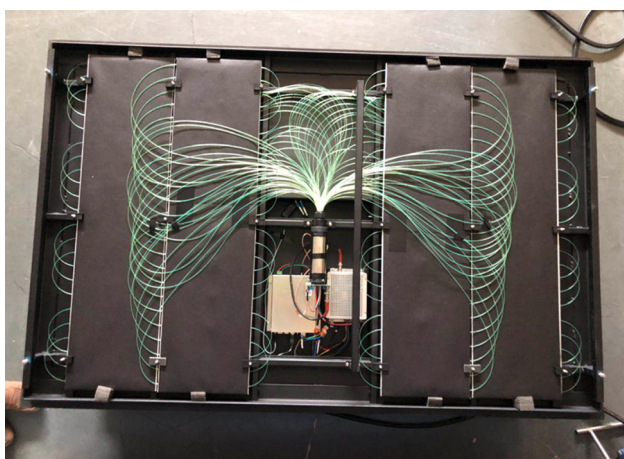


Fig. 2 Photograph of an ED

scheme is designed. An accurate batch test system of the light output is built to test ten units of plastic scintillator units at a time. In this way, an efficient and accurate measurement of each batch is achieved, which can ensure the schedule of the project.

## System setup

The plastic scintillator units we obtained before the test are roughcast. Their four sides need to be cut and polished. The upper and lower surfaces are flat and smooth and do not need to be reprocessed. The machining accuracy requirements are a roughness of less than  $0.2 \mu\text{m}$  and a perpendicularity of less than  $0.5 \text{ mm}$ . The processing quality was tested by a three-coordinate machine and a profiler. The average roughness of a plastic scintillator unit is  $0.098 \mu\text{m}$ , which is equivalent to the N3 grade of roughness. The average perpendicularity is  $0.048 \text{ mm}$ . The roughness and perpendicularity can satisfy the machining accuracy requirements. There is no groove in

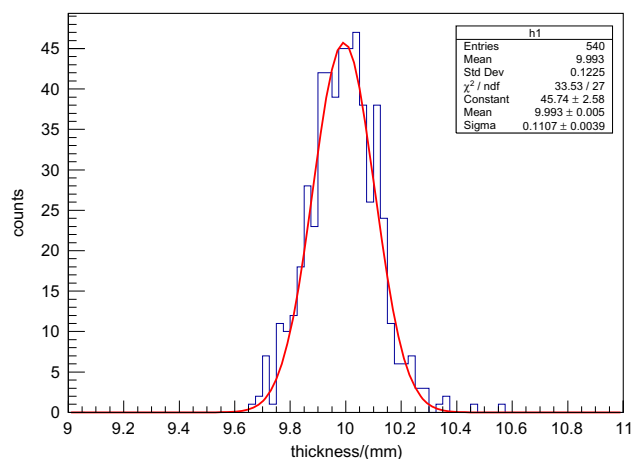


Fig. 3 Distribution of thickness of the scintillator units

the plastic scintillator unit when testing. The thickness of scintillator units among more than 500 units is  $9.993 \text{ mm}$ , as shown in Fig. 3. This result was measured by an ultrasonic thickness gauge (TUM-200T).

The batch test system was built, and its schematic is shown in Fig. 4. The test system is placed at room temperature. There are 4 trigger probes and 10 tested plastic scintillator units in the test system. The probes are placed at the top and bottom layers. P1 and P2 are defined as near probes, which are used to select near events. Similarly, P3 and P4 are defined as far probes to select far events. In the experiment, the probe vertical spacing is  $68.2 \text{ cm}$ . The detection sensitive medium of the probe is a scintillator unit with a size of  $25 \text{ cm} \times 25 \text{ cm} \times 2 \text{ cm}$  (Fig. 5). Eight fiber grooves are evenly distributed on the surface of the scintillator unit, and the distance between two adjacent grooves is  $3.125 \text{ cm}$ . Four WLS fibers with a length of  $2.7 \text{ m}$  pass through the fiber grooves in turn and rewind via other grooves at a distance of 4 grooves. The end faces of the 4 fibers converge into a bundle and are air-coupled to the PMT. This kind of structure has better uniformity of hit positions. To enhance the light collection efficiency, the surface of the scintillator unit is covered with a layer of Tyvek paper. The signal from the PMT is digitized by electronics.

There are 10 detection channels in the middle of the upper and lower probes. The scintillator units to be tested can be fixed in the 10 detection channels. The height of each two adjacent channels is  $5.6 \text{ cm}$ . As shown in Fig. 6, there are ten layers of a push-pull drawer structure to facilitate loading and unloading of the scintillator units. The inner surface of each drawer is painted black to avoid interference from reflected light. At the end of each drawer, a 1.5-in. PMT is fixed vertically so that the center of the short side of the scintillator unit ( $25 \text{ cm}$ ) is directly air-coupled to the PMT, with an air gap of approximately  $1 \text{ mm}$ . The PMT is used to measure the intensity of the light signal, which is generated by ionization of the muons passing through the scintillator unit

**Fig. 4** Schematic of the batch test system

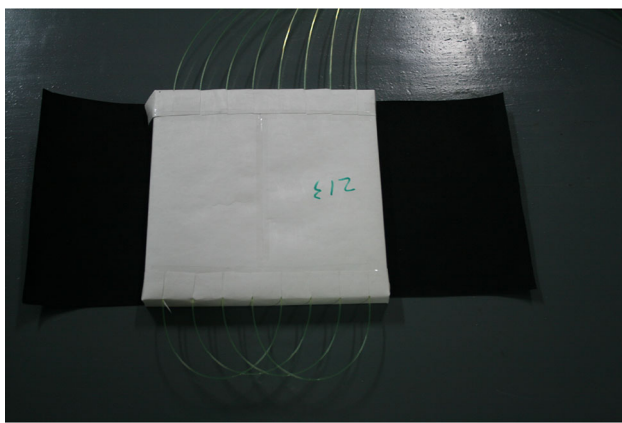
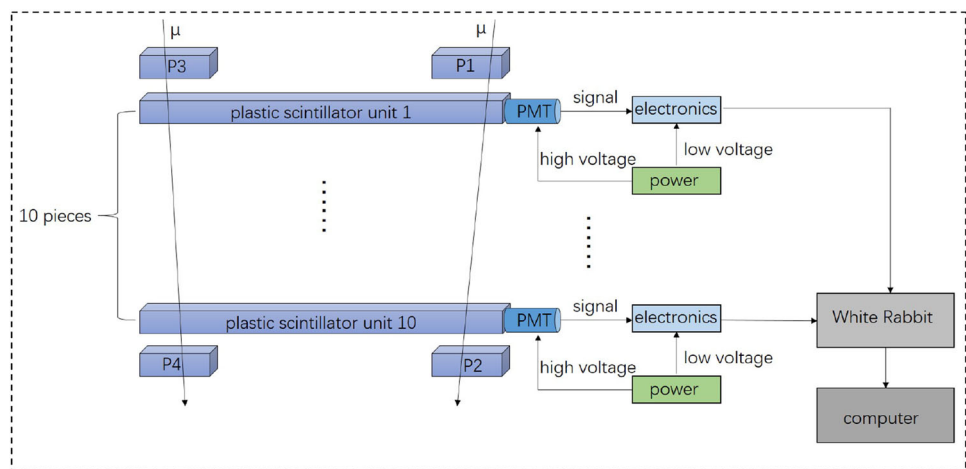


**Fig. 5** Picture of the probe of the batch test system

and then reflected and propagated to the end of one side. The test gain of all 10 PMTs is  $4 \times 10^5$ . The signals exported by the PMTs are transferred to electronics. The electronics can change the charge of the PMT to the ADC count, and the TDC count of the signal arrival time is given at the same time. All timestamps are accurately synchronized within 0.5 ns by the White Rabbit (WR) clock distribution system [11]. The power supply system supplies power to the electronics module and the PMTs. The ED data acquisition system used by the test system can control the trigger mode, data transmission and storage. When a muon passes through any set of telescopes, it may trigger the upper and lower probes. The trigger condition is that the up and down probes are triggered within the 200 ns time window. The signal of the layer under test within 5  $\mu$ s before and after the trigger time is recorded.

The near events are less affected by the plastic scintillator Light Attenuation Length (LAL). We can compare the difference between the light output of different scintillator units by using the near probes. The far events are greatly affected by the plastic scintillator LAL. By measuring the ratio of the sig-



**Fig. 6** Photograph of the batch test system

nals of selected far and near probe events (F/N), the changes in the LAL of plastic scintillator units can be demonstrated.

Since the muon count rate at sea level (laboratory) is approximately  $166 \text{ Hz/m}^2$  and the effective geometric area of detection in each probe is  $0.0625 \text{ m}^2$  ( $25 \text{ cm} \times 25 \text{ cm}$ ), the count rate of two events coinciding in the 200 ns time window is  $4.3 \times 10^{-5} \text{ Hz}$  [12]. Therefore, the probability of more than two muons hitting the scintillator unit at the same time is negligible. Thus, the cosmic ray events triggered

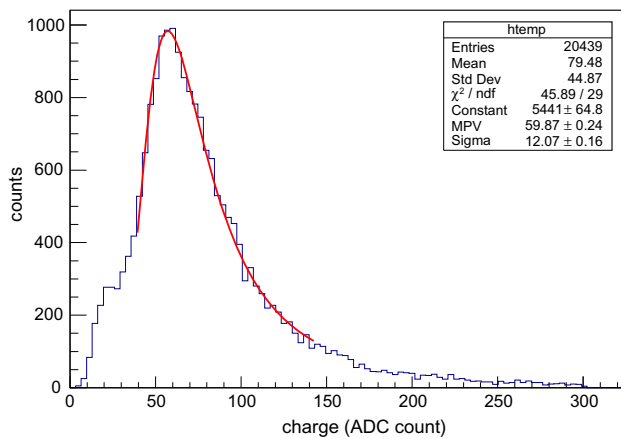


Fig. 7 Distribution of charge spectrum in the case of single muons

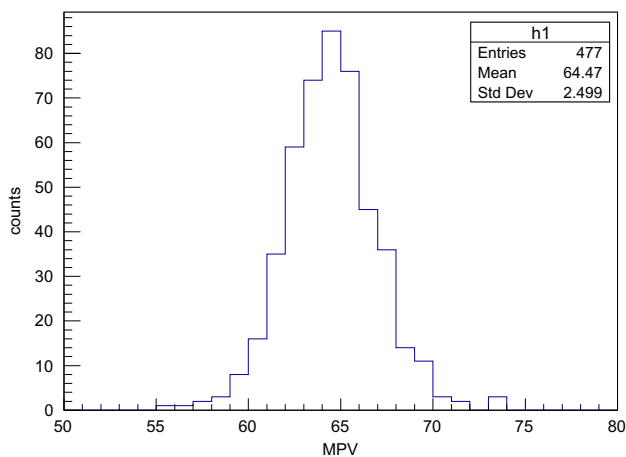


Fig. 8 Distribution of MPVs in the early stage

are mainly single muon events. According to the geometric effect, the trigger rate of near-vertical events is approximately 0.8 Hz. Figure 7 shows the single muon spectrum obtained from 20,000 single muon events of a scintillator unit. Because of the effect of  $\delta$  electrons, the distribution of a single muon spectrum is a Landau distribution. Using the Landau function to fit the charge spectrum, the most probable value (MPV) can be obtained. The MPV is proportional to the light output of the scintillator unit. Therefore, the MPV is used later to characterize the light output of a plastic scintillator. The general test time is 3 h, and there are approximately 8000 events.

## Batch testing and data analysis

### Selection of the sample size

More than 20,000 plastic scintillators will be supplied in batches in 2.5 years. To increase the testing efficiency, a

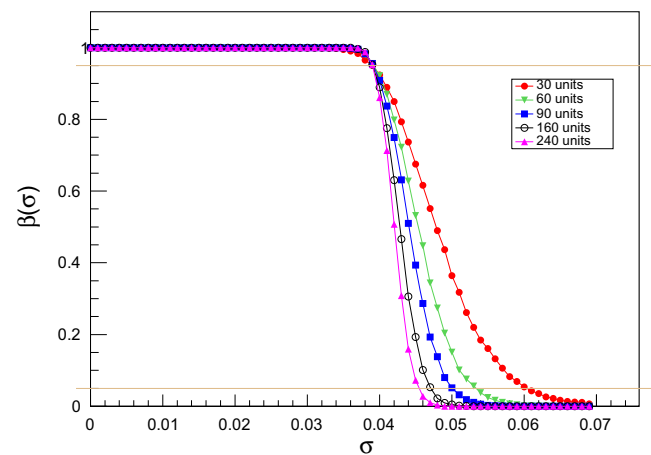


Fig. 9 OC function curves

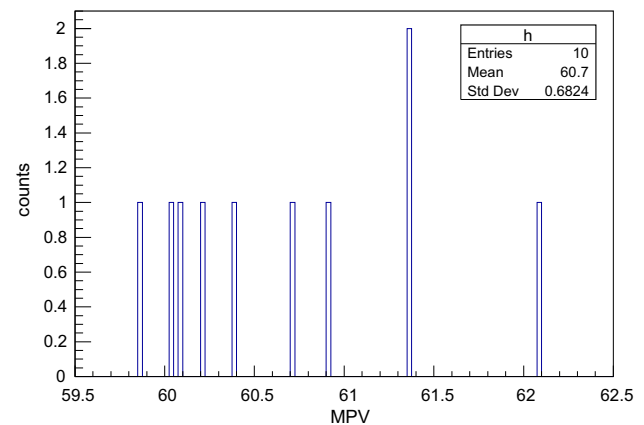


Fig. 10 Distribution of MPVs of one unit

sampling plan is adopted in our experiment. For plastic scintillator units of each batch, the consistency (defined as the relative distribution width: RMS/mean) of the light output should be tested. The  $\chi^2$  test is performed on the relative distribution width of the sample. The consistency of the light output is required to be less than 5% at the 95% confidence level.

Sampling inspection introduces two kinds of wrong judgments: abandoning truth (type A) and accepting falsehood (type B). In type A, a qualified batch is misjudged as a nonqualified batch (producer risk), and the probability of misjudgment is required to be  $\alpha < 5\%$ . In type B, an unqualified batch is mistakenly judged as a qualified batch (user risk), and the probability of misjudgment is required to be  $\beta < 5\%$ . To make the two kinds of wrong judgments small (meaning  $\alpha < 5\%$  and  $\beta < 5\%$ ), the appropriate sample size needs to be calculated.

From the light output test results of more than 400 scintillator units in the early stage, it can be speculated that the width (RMS/Mean) of the overall scintillator unit light output distribution is approximately 3.9% (Fig. 8). A one-tailed



**Table 1** Calibration coefficients

Channel	1	2	3	4	5	6	7	8	9	10
Calibration coefficients	0.946	1.034	0.872	1.113	1.121	1.345	1.587	1.000	0.930	0.944

**Table 2**  $\chi^2$  of two reference plastic scintillator units

	S1	S2
1st channel	6.54	6.99
5th channel	8.95	14.59
8th channel	3.42	10.11

test of the consistency  $\sigma$  can be described as  $H_0 : \sigma \leq \sigma_0$ ,  $H_1 : \sigma > \sigma_0$ . The operating characteristic (OC) function of the  $\chi^2$  test method is:

$$\beta(\sigma) = P_{\sigma}(\text{accepting } H_0) = P_{\sigma}\{(n-1)S^2/\sigma_0^2 < \chi_{\alpha}^2(n-1)\}, \tag{1}$$

where  $\sigma_0$  is 3.9%, S is the standard deviation,  $P_{\sigma}$  is the probability, and n is the number of samples. The receiving probability  $\beta(\sigma)$  (a point in Fig. 9) of different  $\sigma$  was obtained by 10,000 simulations with the  $\chi^2$  test. The OC function curves of 30, 60, 90, 160 and 240 units were simulated. Fixing the sample size and calculating the  $\beta(\sigma)$  of different  $\sigma$  values, five OC function curves were obtained.  $\beta(\sigma)$  is a decreasing function of  $\sigma$ . It is required that when  $\sigma \geq \sigma_0 + \delta$ ,  $\beta(\sigma) \leq 5\%$ .  $\delta$  is chose as 1.1%. Therefore,  $\beta(\sigma_0 + \delta) = 5\%$  is needed. When  $\beta$  is 0.05,  $\sigma$  is no more than 0.05. The OC function curve with a sample size of no less than 90 can meet this requirement.

It is concluded that no less than 90 units should be taken per batch and accepted with a probability of greater than 95% (the probability of abandonment is less than 5%). When the overall consistency of the inspection batch is greater than 5%, it is rejected with a probability of not less than 95% (the pseudo probability is less than 5%). Therefore, the number of each batch is selected according to this requirement.

The selection of the sample size for all batches is processed with a plan of no less than 90 units. Before testing, calibration is implemented. Ten reference scintillator units are tested at the same time, and they are exchanged in turn, realizing testing of each unit in each channel.

The eighth channel is treated as the standard channel. The correction coefficients can eliminate the differences among the ten channels.

**Error estimation**

For one chosen channel, one plastic scintillator unit was placed repeatedly ten times, and the relative fluctuation in

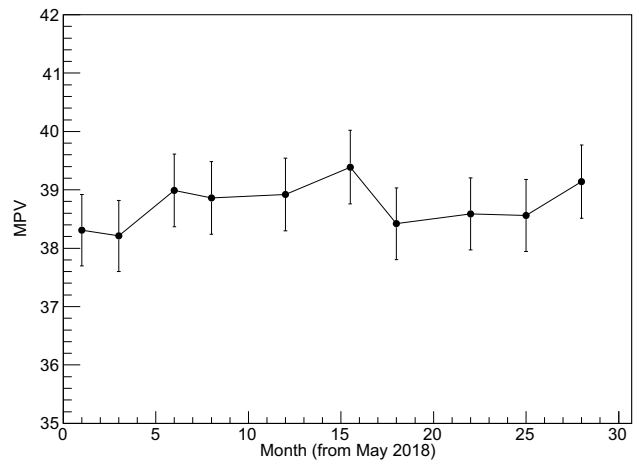


**Fig. 11** Stability result of the long-term monitoring of S1 on the eighth channel

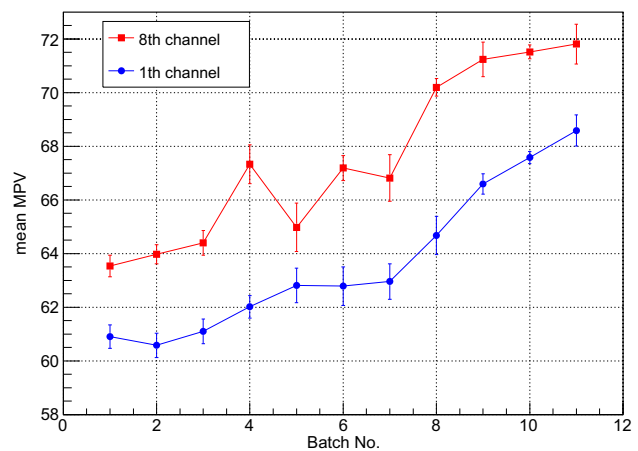


**Fig. 12** Mean MPVs of scintillator in the 1st and 8th channels before calibration

the light output was:

$$\sigma_1 = \text{RMS}/\text{Mean} = 1.1\% \pm 0.3\%, \tag{2}$$

where RMS is 0.68, representing the root mean square of the data, and Mean is 60.7, representing the mean value of the data, which is shown in Fig. 10. Therefore, the error in one measurement is less than 1.4%. The MPV was obtained by fitting. The fitting error is 0.77%, which was obtained by 100 measurements. Therefore, the total error in one measurement is  $\sigma_2 = \sqrt{1.4\%^2 + 0.77\%^2} = 1.6\%$ . The error of the correction factor is  $\sigma_3 = \sqrt{2} \times \sqrt{1.6\% \times \sqrt{10}} = 0.72\%$ . As calculated by the error transfer formula, the relative error

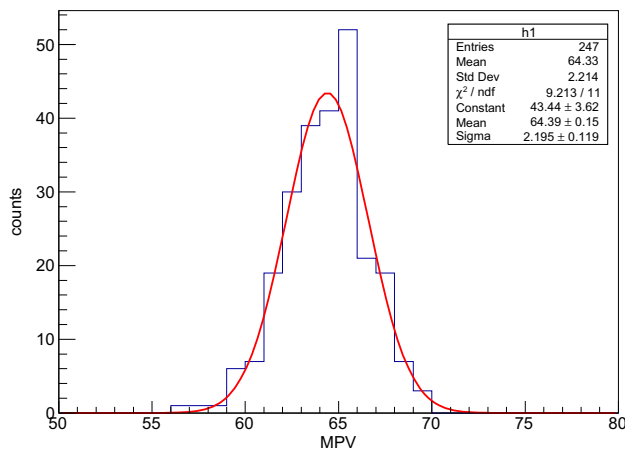


Fig. 13 MPV of the third batch

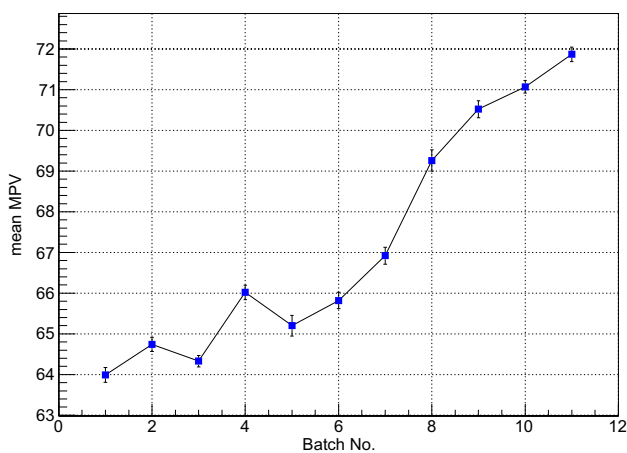


Fig. 14 Results of the whole eleven batches

after each layer of measurement is corrected is:

$$\sigma = \sqrt{\sigma_3^2 + \sigma_2^2} = 1.8\%. \quad (3)$$

## Sample testing and results

There are discrepancies among the MPVs of a single muon spectrum when the same plastic scintillator unit is tested in the ten different channels. They mainly come from the following aspects. Although the test gains of the PMTs in the ten channels are the same, the quantum efficiency of the photocathode and collection efficiency of the photocathode to the first dynode among different PMTs are different. In addition, the widths of the air gaps between the fixed PMTs and the side of the scintillator units are different. The gains among the electronics are also different. To eliminate such inherent inconsistencies of each channel and enable accurate measurement of the differences in the light output performance among scintillator units, the results need to be calibrated.

The calibration coefficients of the ten channels for the first batch are shown in Table 1. The differences in the correction coefficients between different channels are between -13% and 59%. We performed calibrations 10 times in 28 months. The correction factors obtained each time were used for the current batch test.

We performed a  $\chi^2$  test on the MPV of two reference units in channels 1, 5 and 8. For the unilateral test problem (the significance level is  $\alpha$ ), the rejection region is  $\chi^2 = \frac{(n-1)s^2}{\sigma_0^2} = \chi_\alpha^2(n-1)$ , where  $\alpha = 0.05$ ,  $n=10$ ,  $s^2$  is the variance, and  $\sigma_0$  is 1.6% times the average value of the ten numbers; 1.6% is the total error in one measurement (see Sect. 3.2). We know that  $\chi_{0.05}^2(9) = 16.92$  according to the  $\chi^2$  table. When  $\chi^2 < 16.92$ , the MPV is stable. Table 2 shows the  $\chi^2$  of two reference plastic scintillator units. The plastic scintillator unit whose  $\chi^2$  value is less than 16.92 is considered stable. The table shows that for both S1 and S2, the 1st, 5th and 8th channels are stable. Figure 11 shows the stability of S1 in the 8th channel. S1 is stable in the 8th channel. In Fig. 12, the red line represents the mean MPVs of scintillator units tested in the 8th channel, and the blue line represents the mean MPVs of scintillator units tested in the 1st channel. The change trend of the plastic scintillators in the 1st channel is similar to that in the 8th channel. The difference comes from two aspects. One is the difference arising from the channels. The other is the difference arising from the use of different plastic scintillator units of the same batch.

Figure 13 exhibits the distribution of the MPVs of the third batch after calibration. The mean is 64.33, and the RMS/mean is 3.4%. Each batch was similarly processed, and Fig. 14 is obtained from the distribution of each batch. The difference between the maximum and minimum values of the eleven batch averages is approximately 12%. The light output of the plastic scintillator units is improving. Table 3 shows far and near probe test results. As mentioned earlier, at least 90 units will be sampled for each batch for testing. If 90 units are tested, after calculation, if the sampled plastic scintillator inconsistency is less than 4.4%, it can meet the requirements; 240 units were tested in the first batch, and the inconsistency was 4.4%. After calculation, the inconsistency also met the requirements. Therefore, the inconsistency of all batches meets the requirements. The variation in F/N is in the range of 5%, which indicates the change in the LAL of the scintillator units. The results indicate that the LAL of the scintillator units in the last few batches increases. Therefore, the increased light output of the last few batches is also affected by the LAL of the scintillator units.

**Table 3** Test results of different batches

Batch No.	1	2	3	4	5	6	7	8	9	10	11
MPV (near)	63.5	64.0	64.3	66.0	65.2	65.8	66.2	69.3	70.5	71.1	71.9
RMS/Mean (near)	4.4%	3.1%	3.4%	3.0%	3.7%	2.9%	2.9%	3.5%	2.8%	3.0%	2.3%
MPV (far)	47.0	47.5	47.5	48.7	47.0	48.0	48.3	51.8	53.1	53.2	54.5
F/N	0.735	0.733	0.738	0.737	0.720	0.723	0.722	0.748	0.753	0.748	0.757

## Conclusion

A set of reliable and effective samplings was developed, and the consistency of the light output is required to be less than 5% at the 95% confidence level. By building a batch test system, the measurement of large quantities of plastic scintillator units has been realized, and the progress of the project has been ensured. It is confirmed that the quality of the plastic scintillator units is improving.

**Acknowledgements** This work is supported by National Key R&D program of China under the grant 2018YFA0404201, by the National Natural Science Foundation of China (Grant Nos. 11805209, 12022502), the Chinese Academy of Science, Institute of High Energy Physics.

## Declarations

**Conflicts of interest** On behalf of all authors, the corresponding author states that there is no conflict of interest.

## References

- C. Zhen, LHAASO Collaboration, A future project at Tibet: the large high altitude air shower observatory (LHAASO). *Chin. Phys. C* **02**, 249–252 (2010). <https://doi.org/10.1088/1674-1137/34/2/018>
- C. Zhen, LHAASO Collaboration, Status of LHAASO updates from ARGO-YBJ. *Nucl. Instrum. Methods Phys. Res. A* **742**, 95–98 (2014). <https://doi.org/10.1016/j.nima.2013.12.012>
- H. He, LHAASO Collaboration, Design of the LHAASO detectors. *Radiat. Detect. Technol. Methods* **2**(1), 7 (2018). <https://doi.org/10.1007/s41605-018-0037-3>
- F. Aharonian, Q. An, L.X. Bai, Y.X. Bai, Y.W. Bao, D. Bastieri, X.J. Bi, Y.J. Bi, H. Cai et al., LHAASO Collaboration, The observation of the Crab Nebula with LHAASO-KM2A—a performance study. *Chin. Phys. C* **45**(2), 025002 (2021). <https://doi.org/10.1088/1674-1137/abd01b>
- Z. Zhang et al., LHAASO Collaboration, Study on the performance of electromagnetic particle detectors of LHAASO-KM2A. *Nucl. Instrum. Methods Phys. Res. A* **845**, 429–433 (2017). <https://doi.org/10.1016/j.nima.2016.04.079>
- C. Hou et al., LHAASO Collaboration, Finalized design of LHAASO electromagnetic particle detector, in *PoS ICRC2019*, p. 286 (2020)
- X. Zhang et al., LHAASO Collaboration, Batch measurement of attenuation length of wavelength-shifting fibers for LHAASO electromagnetic detectors, in *PoS ICRC2019*, p. 490 (2020)
- Y. Yu et al., LHAASO Collaboration, Characterization of the photomultiplier tube for the LHAASO electromagnetic particle detector, in *PoS ICRC2019*, p. 481 (2020)
- X. Liu et al., Prototype of readout electronics for the LHAASO KM2A electromagnetic particle detectors. *Chin. Phys. C* **40**(7), 076101 (2016). <https://doi.org/10.1088/1674-1137/40/7/076101>
- F. Aharonian et al., [LHAASO], Performance test of the electromagnetic particle detectors for the LHAASO experiment. *Nucl. Instrum. Methods A* **1001**, 165193 (2021). <https://doi.org/10.1016/j.nima.2021.165193>
- W. Pan et al., High resolution distributed time-to-digital converter (TDC) in a White Rabbit network. *Nucl. Instrum. Methods Phys. Res. A* **738**, 13–19 (2014). <https://doi.org/10.1016/j.nima.2013.11.104>
- E. Schroedinger, Rate of n-fold accidental coincidences. *Nature* **153**(3889), 592–593 (1944)